Jpn. J. Pharmacol. **88**, 428 – 435 (2002)

Characteristics of ATP-Induced Current Through $P2X_7$ Receptor in NG108-15 Cells: Unique Antagonist Sensitivity and Lack of Pore Formation

Tomokazu Watano, Isao Matsuoka and Junko Kimura*

Department of Pharmacology, Fukushima Medical University School of Medicine, 1 Hikarigaoka, Fukushima 960-1295, Japan

Received November 14, 2001 Accepted January 7, 2002

ABSTRACT—ATP activates the mouse $P2X_7$ receptor and induces a nonselective-cation current in NG108-15 cells. We investigated the effects of five receptor antagonists on the ATP-induced nonselective-cation current through $P2X_7$ receptor ($I_{NS\cdot P2X7}$) in NG108-15 cells. Nonselective P2 receptor antagonists, RB-2, PPADS and suramin inhibited the $I_{NS\cdot P2X7}$ with IC_{50} values of 4.3, 53 and 40 μM, respectively. However, KN-04, which is a potent antagonist of human $P2X_7$ receptors but is not that of rat $P2X_7$ receptors, had only a weak blocking effect. Furthermore, oxidized-ATP (300 μM), an antagonist of the $P2X_7$ receptor-mediated pore-formation, did not affect the $I_{NS\cdot P2X7}$. Prolonged ATP application did not increase the membrane permeability to large molecules, *N*-methyl-D-glucamine or Yo-Pro-1, indicating that pore-formation was not promoted by the $P2X_7$ receptor activation in NG108-15 cells. These results suggest that antagonist sensitivities and pore-forming properties of the $P2X_7$ receptors in NG108-15 cells are different from those of other cells types.

Keywords: ATP, $P2X_7$ receptor, Antagonist, Pore formation, NG108-15 cell

Extracellular ATP exerts its diverse physiological effects through activation of P2 receptors. P2X receptors are ligand-gated nonselective cation channels and currently seven subtypes ($P2X_{1-7}$) are known (1, 2). $P2X_7$ receptors are unique in several respects compared to other P2X receptors (3, 4). First, while other P2X ($P2X_{1-6}$) receptors are activated by submicromolar concentrations of ATP, the $P2X_7$ receptor requires much higher concentrations (>0.3 mM) of ATP for activation (5). Second, the effective form of ATP that activates the $P2X_7$ receptor is the free base of ATP^{4-} (6) and thus the ATP-induced nonselective-cation current through $P2X_7$ receptor ($I_{NS\cdot P2X7}$) is potentiated by reducing external Mg^{2+} (7). Third, benzoylbenzoic ATP (BzATP) is a more potent agonist than ATP (7 – 9). Fourth, brief stimulation of the $P2X_7$ receptor opens nonselective cation channels, while sustained or repetitive activation of the $P2X_7$ receptor results in the formation of large pores (9, 10), which might be the mechanism of the involvement of the $P2X_7$ receptor in ATP-induced cell death of monocytes and macrophages (11, 12).

NG108-15 cells are hybrids of mouse neuroblastoma N18TG-2 and rat glioma C6Bu-1 cells (13). We previously found that NG108-15 cells express functional $P2X_7$ receptors, which are originated from mouse N18TG-2 cells (7, 14). In NG108-15 cells, the $P2X_7$-receptor agonists BzATP and high concentrations of ATP (>500 μM) open the $P2X_7$ receptor-nonselective cation channels, which lead to a Ca^{2+} influx from the extracellular space and sustained increase in intracellular Ca^{2+} concentration (7, 15, 16).

The $P2X_7$ receptor is inhibited by several compounds, including RB-2, PPADS, suramin (10, 17 – 19), KN-04 (20, 21) and oxidized-ATP (22, 23). The antagonistic effects of these compounds are different among species and they also vary among cell types even within the same species. For example, KN-04 is a potent antagonist of human $P2X_7$ receptor (20, 21), but does not antagonize rat $P2X_7$ receptors (21). In the present study, we investigated the effects of P2 antagonists on the mouse $P2X_7$ receptor current in NG108-15 cells, using the whole cell voltage clamp. We also investigated whether prolonged application of ATP induces pore formation in NG108-15 cells.

MATERIALS AND METHODS

Cell culture

NG108-15 cells were grown in high-glucose Dulbecco's modified Eagle's medium supplemented with 7% fetal

*Corresponding author. FAX: +81-24-548-0575
E-mail: jkimura@fmu.ac.jp

bovine serum, 100 μM hypoxanthine, 0.4 μM aminopterin and 16 μM thymidine at 37°C in a humidified atmosphere of 10% CO_2 and 90% air (24). For electrophysiological study, cells were seeded in 12-well tissue culture plates at a density of 1×10^5 cell/well and cultured for 2 – 3 days until becoming confluent. Before experiments, cells were harvested from each well and dispersed in an experimental chamber.

Electrophysiological study

Electrophysiological experiments were carried out using the whole-cell configuration of the patch-clamp technique (25) as described previously (7, 14, 26). Patch pipettes had a tip resistance of about 2 MΩ when filled with an intracellular solution containing 110 mM CsOH, 30 mM CsCl, 50 mM DL-aspartic acid, 5 mM MgATP, 3 mM $MgCl_2$, 5 mM potassium creatine phosphate, 10 mM EGTA and 20 mM HEPES (adjusted to pH 7.2 with DL-aspartic acid). The cells were dispersed in an experimental chamber perfused with Tyrode solution containing 140 mM NaCl, 5.4 mM KCl, 1.8 mM $CaCl_2$, 1 mM $MgCl_2$, 0.33 mM NaH_2PO_4, 5.5 mM glucose and 5 mM HEPES (adjusted to pH 7.4 with NaOH). The temperature of the external solution was maintained at approximately 37°C by a silicon tube water jacket.

Membrane potentials were controlled by a model CEZ-2300 patch-clamp amplifier (Nihon Kohden, Tokyo). Membrane currents were acquired on-line and subsequently analyzed with a computer (DimensionV333C; Dell, Round Rock, TX, USA) using pCLAMP7 software (Axon, Union City, CA, USA). The current-voltage (I-V) relation was obtained by ramp pulses from a holding potential of −10 mV, initially depolarized to 60 mV, then hyperpolarized to −120 mV, and depolarized back to the holding potential with a speed of 1 V/s. The ramp pulse was applied every 3 s.

All the test agents were added to the superfusate. ATP (1 mM) was applied for 10 – 20 s repetitively with 1-min intervals to induce the $I_{NS\cdot P2X7}$. Although $I_{NS\cdot P2X7}$ did not run-down significantly, we induced the $I_{NS\cdot P2X7}$ at least twice to confirm that the current magnitudes were similar, and then an antagonist (RB-2, PPADS, suramin or KN-04) was applied. After perfusing the antagonist for 30 s, ATP was added. The effect of an antagonist was expressed as a percent inhibition, which was calculated by dividing the $I_{NS\cdot P2X7}$ magnitude in the presence of an antagonist by that just before introducing the antagonist. Since the inhibition by oxidized-ATP required an incubation period of 120 min (27), the current densities were compared between the cells treated with and those without oxidized-ATP. The current density was obtained by dividing the current by the membrane capacitance (Cm). Cm was calculated using the test protocol in pCLAMP7 software with the following equation:

$$Cm = i_c dt/dv$$

where i_c is the capacitive current. Data are expressed as means ± S.E.M. IC_{50} values are determined by probit analysis using EXCEL software and expressed as geometric means with 95% confidence.

To determine whether pore formation of $P2X_7$ receptors occurs, the reversal potential of the $I_{NS\cdot P2X7}$ activated by 3 mM ATP was first measured in the Tyrode solution containing 140 mM Na^+ and then the external solution was changed to one containing 140 mM *N*-methyl-D-glucamine (NMDG) instead of Na^+. The divalent cation concentrations were the same in both solutions.

Yo-Pro-1 uptake

$P2X_7$ receptor-mediated pore formation was also evaluated by uptake of Yo-Pro-1, a fluorescence DNA chelating dye (28). Cells resuspended at $1 – 2 \times 10^6$ cells/ml in the HEPES buffer containing 10 μM Yo-Pro-1 (Molecular Probes, Eugene, OR, USA) were transferred into a 10 × 10 mm quartz cuvette placed in the thermostat-regulated sample chamber of a dual-excitation beam spectrofluorometer (F-2000; Hitachi, Tokyo). Cells was continuously stirred with a circular stir and stimulated with 1 mM ATP at 37°C. The fluorescence change in Yo-Pro-1-containing cell suspension was continuously monitored with an excitation wavelength of 490 nm, and emission of 509 nm. At the end of the experiments, digitonin (50 μg/ml) was added to the cell suspension to obtain maximal fluorescence.

Drugs

ATP (adenosine 5'-triphosphate 2Na; Wako, Osaka) and oxidized-ATP (Sigma, St. Louis, MO, USA) were dissolved in water and diluted with Tyrode solution. The pH was adjusted to 7.4 with NaOH. RB-2 (reactive blue 2) (RBI, Natick, MA, USA), PPADS (pyridoxalphosphate-6-azophenyl-2',4'-disulfonic acid) (Tocris, Bristol, UK), suramin (RBI), KN-04 ([*N*-1-[*N*-methyl-*p*-(5-isoquinolinesulfonyl)benzyl]-2-(4-phenylpiperazine)ethyl]-5-isoquinolinesulfonamide) (Seikagaku Corporation, Tokyo), KN-62 ([1-[*N*,*O*-bis (5-isoquinolinesulfonyl)-*N*-methyl-L-tyrosyl]-4-phenylpiperazine]) (Seikagaku Corporation) were dissolved in dimethylsulfoxide (DMSO) and diluted with Tyrode solution. The final concentration of DMSO was less than 0.1%.

RESULTS

Effects of RB-2, PPADS and suramin on $I_{NS\cdot P2X7}$

We first investigated the effects of the non-selective P2 receptor antagonists, RB-2, PPADS and suramin. RB-2 (3 μM) did not affect the basal current, but it inhibited the $I_{NS\cdot P2X7}$ induced by 1 mM ATP (Fig. 1A). The inhibition by

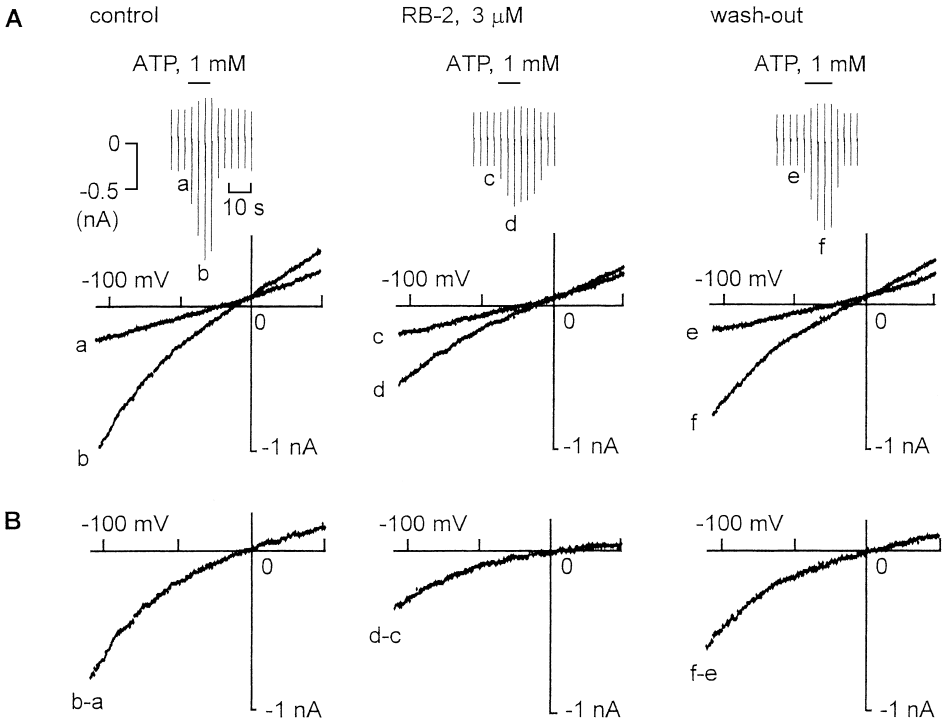

Fig. 1. Effect of RB-2 on the $I_{NS\cdot P2X7}$. A: Typical chart recordings (upper panels) and I-V curves (lower panels) of $I_{NS\cdot P2X7}$ before (left), in the presence of (middle) and after washing out (right) RB-2. ATP was applied during the period shown by the horizontal bars. RB-2 (3 μM) was applied 30 s before ATP application. B: Difference I-V curves obtained by subtracting the control from the maximal current response to ATP at each trace in A, indicating net $I_{NS\cdot P2X7}$. Labels correspond to those in A.

RB-2 was almost fully reversed after washing out the drug for 2 min (Fig. 1A). Figure 1B shows the I-V curves of the net $I_{NS\cdot P2X7}$ obtained by subtracting the control current from the current in the presence of ATP before (left), in the presence of (middle) and after washing out (right) RB-2. The I-V curves of the $I_{NS\cdot P2X7}$ showed a slight inward rectification at the negative potentials.

PPADS (100 μM) and suramin (100 μM) were tested using the same protocol as that for RB-2 and the results are shown in Figs. 2 and 3, respectively. These two antagonists also inhibited the $I_{NS\cdot P2X7}$ and the inhibition was also completely reversed after washing out the drugs for 1 min.

Concentration-inhibition curves for the three antagonists were plotted by measuring the net $I_{NS\cdot P2X7}$ at −100 mV (Fig. 4). The inhibitory effects of RB-2, PPADS and suramin were concentration-dependent with IC_{50} (geometric means with 95% confidence intervals) values of 4.3 (3.0 – 5.9), 53 (25 – 81) and 40 (26 – 60) μM, respectively. The data with RB-2, PPADS and suramin could be fit with Hill coefficients of 0.76, 1.8 and 2.4, respectively.

Effect of KN-04 on $I_{NS\cdot P2X7}$

A Ca^{2+}-calmodulin-dependent protein kinase II inhibitor, KN-62, and its inactive analogue, KN-04, in nanomolar concentrations inhibit human $P2X_7$ receptor-mediated responses (20, 21). In NG108-15 cells, the $I_{NS\cdot P2X7}$ was little affected by 1 μM KN-04, which totally inhibits the human $P2X_7$ receptor-mediated effect (Fig. 5). Even at 10 μM, KN-04 only decreased $I_{NS\cdot P2X7}$ to 61.3 ± 9.5% (n = 4) of the control value. The inhibition was reversible, as the current almost fully recovered after washing out KN-04 for 1 min.

Effect of oxidized-ATP on $I_{NS\cdot P2X7}$

Oxidized-ATP is an irreversible inhibitor of the P2Z receptor in human lymphocytes (22) and of the cloned expressed human $P2X_7$ receptor (9). We incubated NG108-15 cells with 300 μM oxidized-ATP for 120 min, and compared the $I_{NS\cdot P2X7}$ densities between oxidized-ATP-treated and non-treated cells. When $I_{NS\cdot P2X7}$ was induced by ATP concentrations between 0.5 and 5 mM, no difference was found between the current in the oxidized-ATP-treated cells and that in non-treated cells (Fig. 6). This indicates that oxidized-ATP does not inhibit the $P2X_7$ receptor in NG108-15 cells.

Effect of prolonged ATP application on $P2X_7$ receptors

The inhibitory effects of oxidized-ATP on the $P2X_7$ receptor have been demonstrated with ATP-induced cell lysis and pore formation (23, 27) but not with the membrane current. The failure of oxidized-ATP to inhibit the

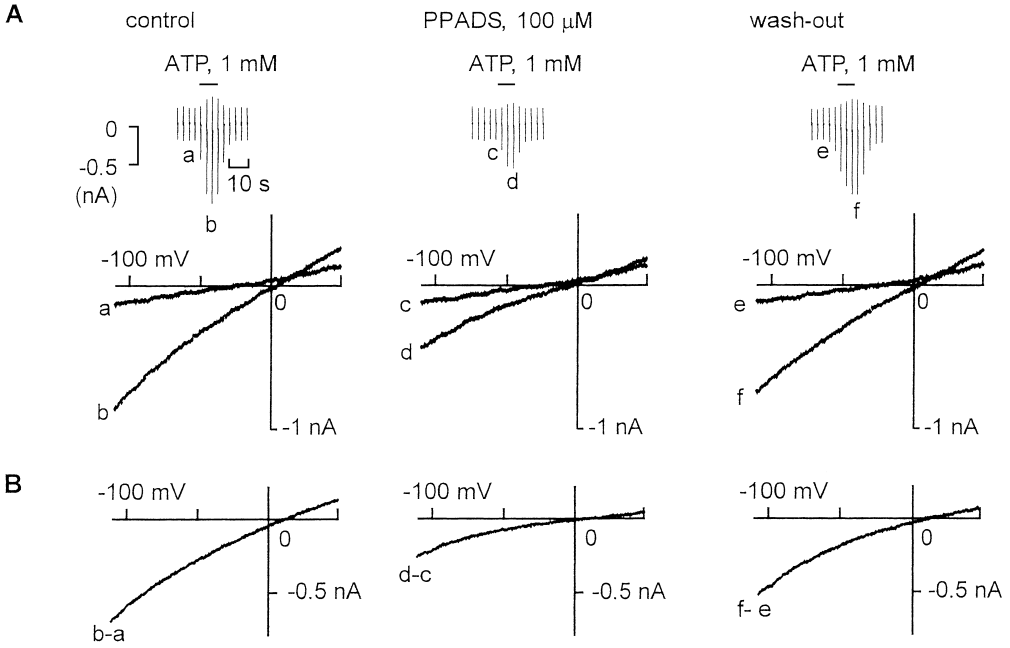

Fig. 2. Effect of PPADS on the $I_{NS\cdot P2X7}$. A: Typical chart recordings (upper panels) and I-V curves (lower panels) of $I_{NS\cdot P2X7}$ before (left), in the presence of (middle) and after washing out (right) PPADS. ATP was applied during the period shown by the horizontal bars. PPADS (100 μM) was applied 30 s before ATP application. B: Difference I-V curves obtained by subtracting the control from the maximal current response to ATP at each trace in A.

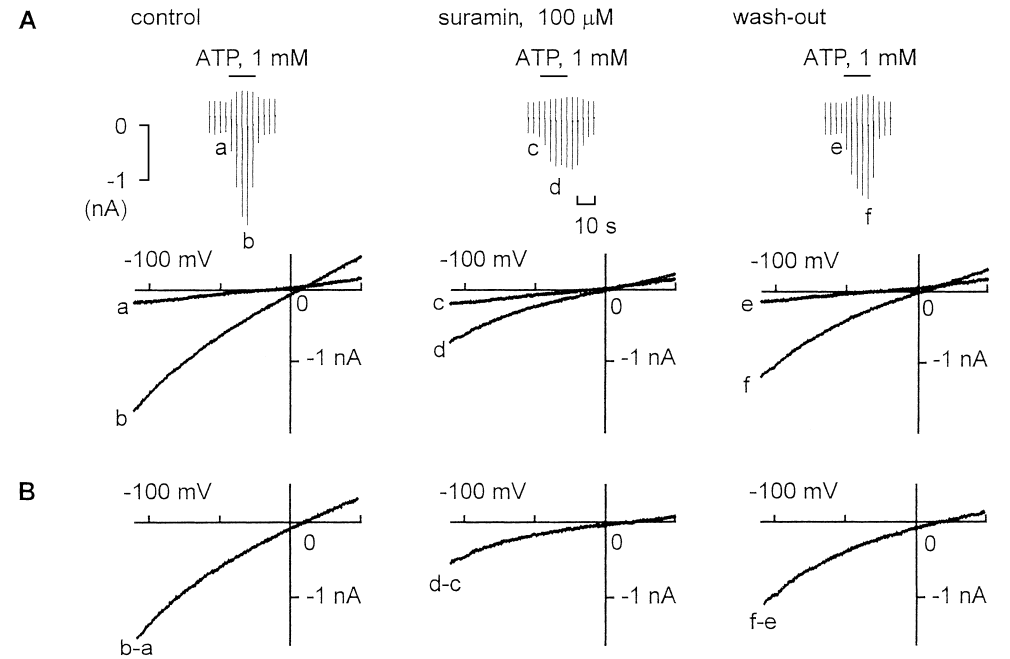

Fig. 3. Effect of suramin on the $I_{NS\cdot P2X7}$. A: Typical chart recordings (upper panels) and I-V curves (lower panels) of $I_{NS\cdot P2X7}$ before (left), in the presence of (middle) and after washing out (right) suramin. ATP was applied during the period shown by the horizontal bars. Suramin (100 μM) was applied 30 s before ATP application. B: Difference I-V curves obtained by subtracting the control from the maximal current response to ATP at each trace in A.

ATP-induced current in NG108-15 cells suggested that the pore-forming ability of P2X$_7$ receptor in these cells are different from that in other cells. Therefore, using the whole cell clamp, we investigated whether P2X$_7$ receptor activation induces pore formation in NG108-15 cells. Figure 7A shows the current activated by 3 mM ATP

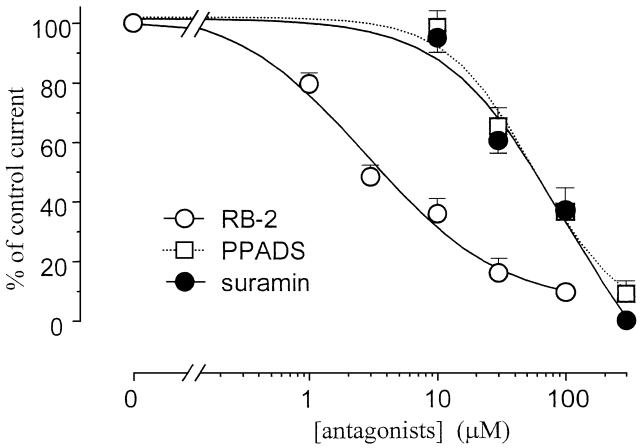

Fig. 4. Concentration-inhibition relationships of RB-2, PPADS and suramin. $I_{NS\cdot P2X7}$ magnitude was measured at −100 mV. $I_{NS\cdot P2X7}$s in the presence of inhibitors are expressed as % of the control in the absence of the inhibitors. Each point represents the mean ± S.E.M. from 3 to 7 cells.

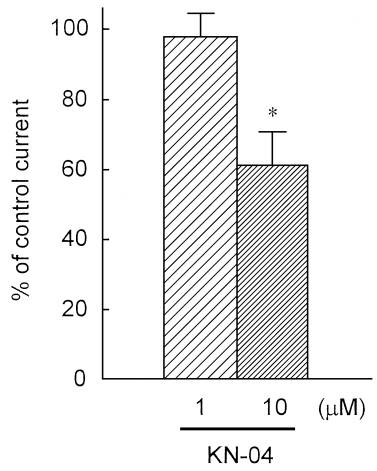

Fig. 5. Effects of 1 and 10 μM KN-04 on $I_{NS\cdot P2X7}$. Current amplitudes were measured at −100 mV. Each column indicates the mean ± S.E.M. from 4 cells. *P<0.01 compared with the control by the Dunnett's test.

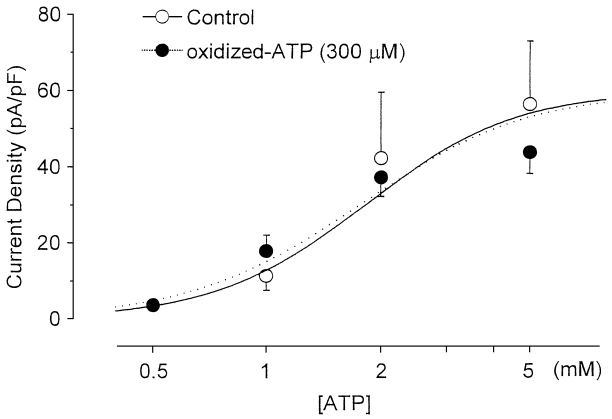

Fig. 6. Effect of oxidized-ATP on the $I_{NS\cdot P2X7}$. The $I_{NS\cdot P2X7}$ density was measured at −100 mV in untreated cells and cells treated with oxidized-ATP. Each symbol represents the mean ± S.E.M. from 4 control and 5 oxidized-ATP treated cells.

applied for 5 min. During this continuous superfusion of ATP, the current did not increase and its reversal potential did not change in Tyrode solution containing 140 mM Na^+ (Fig. 7: B and C). Figure 7D shows a similar experiment in which the external solution was switched from one containing 140 mM Na^+ to one containing 140 mM NMDG about 30 s after starting the application of ATP. Upon substituting Na^+ with NMDG, the current magnitude suddenly decreased and the reversal potential shifted from 5 mV to −55 mV (Fig. 7E). The decreased current remained almost the same during the following 6 min of ATP superfusion in the NMDG solution. When the external solution was changed from one containing NMDG back to one containing Na^+ in the presence of ATP, the current magnitude and the reversal potential were restored nearly to their initial value. These results indicate that prolonged stimulation with ATP does not promote the $P2X_7$ receptors to form pores large enough for the permeation of NMDG and Na equally into NG108-15 cells.

We examined whether Yo-Pro-1 uptake occurs during $P2X_7$ receptor stimulation in NG108-15 cells. ATP (1 mM) did not increase Yo-Pro-1 fluorescence during a 4 min-exposure (Fig. 8). In contrast, membrane disruption by digitonin (50 μg/ml) markedly increased Yo-Pro-1 fluorescence (Fig. 8). Yo-Pro-1 or ethidium bromide uptake through the $P2X_7$ receptors is reported to be facilitated at low concentrations of external divalent cations (9, 29). However, in our experiment, even in a low divalent cation-medium (Mg^{2+}-free and 0.18 mM $CaCl_2$), ATP was unable to stimulate the Yo-Pro-1 uptake in NG108-15 cells (data not shown). This result also indicates that large pores were not formed in NG108-15 cells by prolonged application of ATP.

DISCUSSION

$P2X_7$ receptor stimulation has been reported to lead to two types of molecular responses, namely the opening of intrinsic nonselective cation channels and the formation of large pores, resulting in diverse cellular reactions such as Ca^{2+} influx, uptake of large molecules, cytokine release, activation of phospholipase D, shedding L-selectin from the cell surface, and cell lysis (23, 27, 30, 31). Our results demonstrated that the ATP-induced current through the $P2X_7$ receptor activation in NG108-15 cells had unique antagonist sensitivity compared with those in other cell types, and that prolonged stimulation of the $P2X_7$ receptor did not induce pore formation in NG108-15 cells.

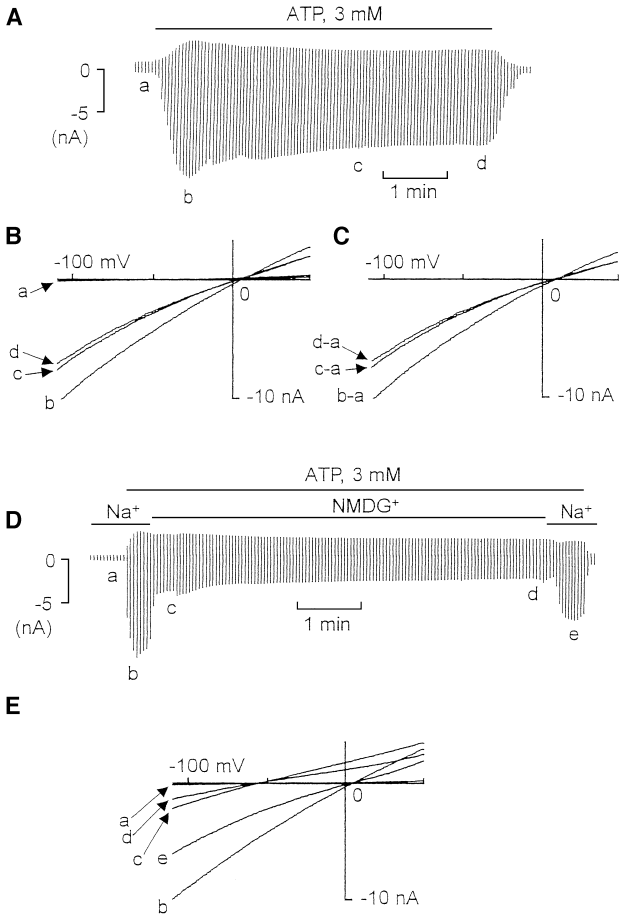

Fig. 7. Effects of prolonged application of ATP on the $I_{NS\cdot P2X7}$ with Na^+ or NMDG in the external solutions. A: Typical chart recording of the $I_{NS\cdot P2X7}$ induced by 3 mM ATP in Tyrode solution containing 140 mM Na^+. The horizontal bars above indicate when ATP was present. B. I-V curves before ATP application (a), maximum current induced by ATP (b), after 3 min (d) and 5 min (d) as indicated in A. C: Difference I-V curves of b-a, c-a and d-a in B. D: Typical chart recording of the $I_{NS\cdot P2X7}$ induced by 3 mM ATP in Tyrode solution containing 140 mM Na^+ or 140 mM NMDG. The horizontal bars above indicate when ATP, Na^+ and NMDG were present. E: I-V curves before ATP application (a), maximum current induced by ATP (b), just after changing to NMDG (c), after 5 min in NMDG (d) and after returning to Na^+ (e) as indicated in D.

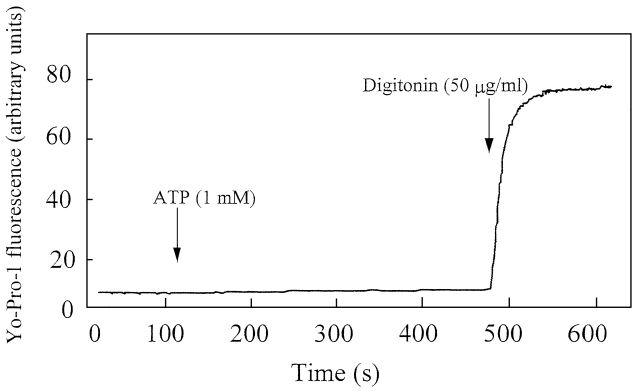

Fig. 8. Effect of ATP on Yo-Pro-1 fluorescence. ATP (1 mM) and digitonin (50 μg/ml) were added as indicated (arrows) while Yo-Pro-1 uptake in NG108-15 cells was measured by fluorescence. No uptake was detected with ATP, but significant fluorescence was detected with digitonin.

In NG108-15 cells, RB-2 was more potent than PPADS and suramin. The IC_{50} values of RB-2, PPADS and suramin were 4.3, 53 and 40 μM, respectively. This order of potency is different from that with human $P2X_7$ receptors because PPADS is more potent (IC_{50} = 1 μM) than suramin (IC_{50} = 70 μM) in inhibiting the human $P2X_7$ receptor current in HEK-293 cells (18). The $I_{NS\cdot P2X7}$ from NTW8 microglial cells is more sensitive to RB-2 than PPADS (29), which is similar to our results with NG108-15 cells. Thus, the difference noted above may be due to the species differences because the $P2X_7$ receptors in both NG108-15 and NTW8 cells are from mouse origin (26). The Hill coefficient of RB-2, is close to 1, while those of PPADS and suramin are greater than 1, indicating that one molecule of RB-2 and more than one molecule of PPADS and suramin may be involved in the inhibition of one functional $P2X_7$ receptor.

Chessell et al. (29) observed no effect of 100 μM suramin on the rising phase of the current in mouse NTW8 cells when they applied ATP for only 0.5 s with their quick solution change method. In contrast, we observed that suramin considerably diminished the initial rising state of the $I_{NS\cdot P2X7}$ and greatly inhibited the maximal current 10 – 20 s after ATP application. It is likely that the $P2X_7$ receptors differ in different cell lines even though the cell lines originated from the same species. However the possibility that the discrepancy is due to the different methods of ATP application can not be excluded.

Unlike other P2X receptor subtypes, several selective antagonists have been found for the $P2X_7$ receptors. The calmodulin kinase II inhibitor KN-62 and its ineffective analogue KN-04 inhibit the human lymphocyte $P2X_7$-receptor-mediated Ba^{2+} influx and ethidium uptake at nanomolar concentrations (20), but did not affect the responses mediated through the rat P2X7 receptors (30). Human and rat $P2X_7$ receptors have 80% homology in amino acid sequences (21). Introduction of the first 335 amino acids of the human $P2X_7$ receptor to the rat $P2X_7$ receptor conferred KN-62 sensitivity (21), suggesting that the drug interacts with residues in the amino-terminal half of the human $P2X_7$ receptor which contains the large extracellular loop. In NG108-15 cells, KN-04 at 1 μM had no effect and it only partly inhibited the $I_{NS\cdot P2X7}$ at 10 μM. Similar weak inhibition was found for KN-62. These results can not be explained by species differences, because KN-62 inhibits both native and recombinant mouse $P2X_7$ receptors from

the NTW8 microglial cell line with IC_{50}s of 1.17 μM and 180 nM, respectively (31). A significant difference was also obtained with oxidized-ATP, another selective blocker of human, rat and mouse $P2X_7$ receptors (22, 23, 27, 32). Oxidized-ATP had no effect on the $I_{NS\cdot P2X7}$ in NG108-15 cells. This also cannot be explained by species differences. However, it should be noted that the effects of KN-62 (33) and oxidized-ATP (27) on mouse $P2X_7$ receptors were demonstrated with ATP-induced pore formation, but not with the activation by ATP of non-selective cation channels. Several lines of evidence suggest that the induction of non-selective cationic current does not always correlate with pore formation. In recombinant human $P2X_7$ receptors, PPADS inhibits ATP-induced pore formation with an IC_{50} of 15 nM, while inhibition of the current requires a 100-fold higher concentration of PPADS (18). Calmidazolium inhibits the rat $P2X_7$ receptor current without affecting pore formation (34). In addition, the rat $P2X_7$ receptor expressed in *Xenopus* oocytes does not form a pore (35). Therefore, channel activation and pore formation appear to be separate events that are affected differently by KN-compounds and oxidized-ATP.

With respect to the $P2X_7$ receptor pore formation, our results suggest that prolonged stimulation of the $P2X_7$ receptor did not induce pore formation in NG108-15 cells. The $P2X_7$ receptor in NG108-15 cells is less permeable to NMDG than to Na^+ (7). The rat $P2X_7$ receptor in macrophages, which has a marked pore forming activity, is equally permeable to NMDG and Na^+ (35). In addition, Khakh et al. (36) and Virginio et al. (37) showed that prolonged activation of $P2X_2$ and $P2X_4$ receptors progressively increased their permeability to NMDG and proposed a pore dilatation property for these P2X receptor subtypes. We did not observe such a change in the permeability to NMDG in NG108-15 cells during the application of 3 mM ATP for 6 min. Pore formation was facilitated at low concentrations of divalent cations, but also occurred in normal divalent cations at 32°C in mouse NTW8 microglial cells (29). Yo-Pro-1 uptake was observed at 1 mM $CaCl_2$ at 37°C in the mouse $P2X_7$ receptor in HEK-293 cells and in the native NTW8 cells (33). In this study, we showed that prolonged stimulation of the $P2X_7$ receptor in NG108-15 cells did not incraese Yo-Pro-1 uptake even in a low divalent cations-medium. Thus, we conclude that the mouse $P2X_7$ receptors in NG108-15 cells do not form large pores. These results might be related to the lack of effects of KN-04 and oxidized-ATP in NG108-15 cells.

An alternative explanation for the different sensitivities to antagonists and lack of pore formation in NG108-15 cells would be that some other cellular protein is either deficient or present in these cells that alters the properties of the $P2X_7$ channels. Another possibility is that the $P2X_7$ receptor may be heteromeric. Heteromeric P2X receptors have been demonstrated as combinations of $P2X_2$ and $P2X_3$ (38, 39), $P2X_1$ and $P2X_5$ (40), and $P2X_4$ and $P2X_6$ receptor subtypes (41). In NG108-15 cells, considerable levels of mRNAs for $P2X_3$ and $P2X_4$ receptors were detected (I. Matsuoka, unpublished data). However, we could not measure any membrane current at lower concentrations of ATP, which is an indication that homomeric P2X3 or P2X4 receptors are not expressed in these cells. The interaction between these P2X receptor subtypes and the $P2X_7$ receptor would be an important subject for future study.

Acknowledgments

We thank Professor T. Shimizu, Department of Physiology, Fukushima Medical University School of Medicine, for permitting us to use the patch-clamp apparatus in his department. We also thank Ms S. Sato and Dr. T. Ono for their technical assistance. This work was supported by the Japan Health Science Foundation (21279), the Smoking Research Foundation, and Grants-in-Aid for Scientific Research from the Ministry of Education, Culture, Sports, Science and Technology of Japan (11770047, 11670096, 11357020).

REFERENCES

1 Valera S, Hussy N, Evans RJ, Adami N, North RA, Surprenant A and Buell G: A new class of ligand-gated ion channel defined by P2x receptor for extracellular ATP. Nature **371**, 516 – 519 (1994)
2 Brake AJ, Wagenbach MJ and Julius D: New structural motif for ligand-gated ion channels defined by an ionotropic ATP receptor. Nature **371**, 519 – 523 (1994)
3 Kimura J, Kaiho H and Matsuoka I: P2Z/$P2X_7$, receptor (a review). Recent Res Dev Neurochem **2**, 241 – 246 (1999)
4 Nihei OK, Savino W and Alves LA: Procedures to characterize and study P2Z/$P2X_7$ purinoceptor: flow cytometry as a promising practical, reliable tool. Mem Inst Oswaldo Cruz **95**, 415 – 428 (2000)
5 North RA and Barnard EA: Nucleotide receptors. Curr Opin Neurobiol **7**, 346 – 357 (1997)
6 Cockcroft S and Gomperts BD: The ATP4-receptor of rat mast cells. Biochem J **188**, 789 – 798 (1980)
7 Kaiho H, Kimura J, Matsuoka I, Kumasaka T and Nakanishi H: ATP-activated nonselective cation current in NG108-15 cells. J Neurochem **67**, 398 – 406 (1996)
8 Burnstock G: The past, present and future of purine nucleotides as signalling molecules. Neuropharmacology **36**, 1127 – 1139 (1997)
9 Surprenant A, Rassendren F, Kawashima E, North RA and Buell G: The cytolytic P2Z receptor for extracellular ATP identified as a P2X receptor ($P2X_7$). Science **272**, 735 – 738 (1996)
10 Rassendren F, Buell GN, Virginio C, Collo G, North RA and Surprenant A: The permeabilizing ATP receptor, $P2X_7$. Cloning and expression of a human cDNA. J Biol Chem **272**, 5482 – 5486 (1997)
11 Chiozzi P, Murgia M, Falzoni S, Ferrari D and Di Virgilio F: Role of the purinergic P2Z receptor in spontaneous cell death in J774 macrophage cultures. Biochem Biophys Res Commun **218**, 176 – 181 (1996)
12 Di Virgilio F: The P2Z purinoceptor: an intriguing role in immunity, inflammation and cell death. Immunol Today **16**, 524 – 528

(1995)
13 Matsuoka I, Zhou Q, Ishimoto H and Nakanishi H: Extracellular ATP stimulates adenylyl cyclase and phospholipase C through distinct purinoceptors in NG108-15 cells. Mol Pharmacol **47**, 855 – 862 (1995)
14 Kaiho H, Matsuoka I, Kimura J and Nakanishi H: Identification of $P2X_7$ (P2Z) receptor in N18TG-2 cells and NG108-15 cells. J Neurochem **70**, 951 – 957 (1998)
15 Chueh SH and Kao LS: Extracellular ATP stimulates calcium influx in neuroblastoma × glioma hybrid NG108-15 cells. J Neurochem **61**, 1782 – 1788 (1993)
16 Chueh SH, Hsu LS and Song SL: Two distinct ATP signaling mechanisms in differentiated neuroblastoma × glioma hybrid NG108-15 cells. Mol Pharmacol **45**, 532 – 539 (1994)
17 Wiley JS, Chen R and Jamieson GP: The ATP^{4-} receptor-operated channel (P2Z class) of human lymphocytes allows Ba^{2+} and $ethidium^{+}$ uptake: inhibition of fluxes by suramin. Arch Biochem Biophys **305**, 54 – 60 (1993)
18 Chessell IP, Michel AD and Humphrey PP: Effects of antagonists at the human recombinant $P2X_7$ receptor. Br J Pharmacol **124**, 1314 – 1320 (1998)
19 McMillian MK, Soltoff SP, Cantley LC, Rudel R and Talamo BR: Two distinct cytosolic calcium responses to extracellular ATP in rat parotid acinar cells. Br J Pharmacol **108**, 453 – 461 (1993)
20 Gargett CE and Wiley JS: The isoquinoline derivative KN-62 a potent antagonist of the P2Z-receptor of human lymphocytes. Br J Pharmacol **120**, 1483 – 1490 (1997)
21 Humphreys BD, Virginio C, Surprenant A, Rice J and Dubyak GR: Isoquinolines as antagonists of the $P2X_7$ nucleotide receptor: high selectivity for the human versus rat receptor homologues. Mol Pharmacol **54**, 22 – 32 (1998)
22 Wiley JS, Chen JR, Snook MB and Jamieson GP: The P2Z-purinoceptor of human lymphocytes: actions of nucleotide agonists and irreversible inhibition by oxidized ATP. Br J Pharmacol **112**, 946 – 950 (1994)
23 Zoetewij JP, van de Water B, de Bont HJ and Nagelkerke JF: The role of a purinergic P2z receptor in calcium-dependent cell killing of isolated rat hepatocytes by extracellular adenosine triphosphate. Hepatology **23**, 858 – 865 (1996)
24 Ohkubo S, Kimura J and Matsuoka I: Correlation between adenine nucleotide-induced cyclic AMP elevation and extracellular adenosine formation in NG108-15 cells. Jpn J Pharmacol **84**, 325 – 333 (2000)
25 Hamill OP, Marty A, Neher E, Sakmann B and Sigworth FJ: Improved patch-clamp techniques for high-resolution current recording from cells and cell-free membrane patches. Pflugers Arch **391**, 85 – 100 (1981)
26 Kaiho H, Kimura J, Matsuoka I and Nakanishi H: Effects of anions on ATP-activated nonselective cation current in NG108-15 cells. J Neurophysiol **77**, 2717 – 2722 (1997)
27 Murgia M, Hanau S, Pizzo P, Rippa M and Di Virgilio F: Oxidized ATP. An irreversible inhibitor of the macrophage purinergic P2Z receptor. J Biol Chem **268**, 8199 – 8203 (1993)
28 Hickman SE, el Khoury J, Greenberg S, Schieren I and Silverstein SC: P2Z adenosine triphosphate receptor activity in cultured human monocyte- derived macrophages. Blood **84**, 2452 – 2456 (1994)
29 Chessell IP, Michel AD and Humphrey PP: Properties of the pore-forming $P2X_7$ purinoceptor in mouse NTW8 microglial cells. Br J Pharmacol **121**, 1429 – 1437 (1997)
30 Humphreys BD and Dubyak GR: Induction of the P2z/$P2X_7$ nucleotide receptor and associated phospholipase D activity by lipopolysaccharide and IFN-gamma in the human THP-1 monocytic cell line. J Immunol **157**, 5627 – 5637 (1996)
31 Chen JR, Gu BJ, Dao LP, Bradley CJ, Mulligan SP and Wiley JS: Transendothelial migration of lymphocytes in chronic lymphocytic leukaemia is impaired and involved down-regulation of both L-selectin and CD23. Br J Haematol **105**, 181 – 189 (1999)
32 Falzoni S, Munerati M, Ferrari D, Spisani S, Moretti S and Di Virgilio F: The purinergic P2Z receptor of human macrophage cells. Characterization and possible physiological role. J Clin Invest **95**, 1207 – 1216 (1995)
33 Chessell IP, Simon J, Hibell AD, Michel AD, Barnard EA and Humphrey PP: Cloning and functional characterisation of the mouse $P2X_7$ receptor. FEBS Lett **439**, 26 – 30 (1998)
34 Virginio C, Church D, North RA and Surprenant A: Effects of divalent cations, protons and calmidazolium at the rat $P2X_7$ receptor. Neuropharmacology **36**, 1285 – 1294 (1997)
35 Nuttle LC and Dubyak GR: Differential activation of cation channels and non-selective pores by macrophage P2z purinergic receptors expressed in *Xenopus* oocytes. J Biol Chem **269**, 13988 – 13996 (1994)
36 Khakh BS, Bao XR, Labarca C and Lester HA: Neuronal P2X transmitter-gated cation channels change their ion selectivity in seconds. Nat Neurosci **2**, 322 – 330 (1999)
37 Virginio C, MacKenzie A, Rassendren FA, North RA and Surprenant A: Pore dilation of neuronal P2X receptor channels. Nat Neurosci **2**, 315 – 321 (1999)
38 Radford KM, Virginio C, Surprenant A, North RA and Kawashima E: Baculovirus expression provides direct evidence for heteromeric assembly of $P2X_2$ and $P2X_3$ receptors. J Neurosci **17**, 6529 – 6533 (1997)
39 Virginio C, North RA and Surprenant A: Calcium permeability and block at homomeric and heteromeric $P2X_2$ and $P2X_3$ receptors, and P2X receptors in rat nodose neurones. J Physiol (Lond) **510**, 27 – 35 (1998)
40 Torres GE, Haines WR, Egan TM and Voigt MM: Co-expression of $P2X_1$ and $P2X_5$ receptor subunits reveals a novel ATP-gated ion channel. Mol Pharmacol **54**, 989 – 993 (1998)
41 Le KT, Babinski K and Seguela P: Central $P2X_4$ and $P2X_6$ channel subunits coassemble into a novel heteromeric ATP receptor. J Neurosci **18**, 7152 – 7159 (1998)